Energy Proceedings
Vol 52, 2025
ISSN 2004-2965

# A Novel Graphical Expression Method for Thermodynamic Systems under Dynamic Boundary Conditions #

Kunteng Huang[1], Ruihua Chen[1], Weicong Xu[1], Shuai Deng[1], Li Zhao[1,*]

1 State Key Laboratory of Engines, Tianjin University, Tianjin 300072, China

(Corresponding Author: jons@tju.edu.cn)

**ABSTRACT**

Graphical methods are among the techniques for quantitatively describing energy conversion processes, which also serve as an important technical pathway to improve energy conversion efficiency. For a thermodynamic system with dynamic boundary conditions, it is challenging to comprehensively describe the energy conversion process using existing graphical methods. To fill this gap, this study proposes a new graphical method called an Energy-Energy (*E-E*) diagram, which employs different energy forms (thermodynamic process parameters) as the axes and is capable of representing dynamic performance variations through the geometric parameters. The applicability of the *E-E* diagram is demonstrated through a case study of an organic Rankine cycle (ORC) system under finite heat capacity boundary conditions. The results show that the *E-E* diagram can not only present the system performance parameters related to both the 1st and 2nd Laws of Thermodynamics but also illustrate the global and local performance of energy conversion process. A significant advantage in describing system thermal performance variation and irreversible losses distribution can be obtained when combined both *E-E* diagram and *T*-s diagram. Moreover, the performance differences between two systems with different boundary conditions can be revealed intuitively through the *E-E* diagram. The *E-E* diagram proposed in this study pioneers the application of process quantities as thermodynamic coordinates, providing a novel graphical method for characterizing the performance of dynamic systems.

**Keywords:** graphical method, energy conversion, thermodynamic process parameter, finite heat capacity;

**NONMENCLATURE**

| | |
|---|---|
| *Abbreviations* | |
| ORC | Organic Rankine Cycle |
| *Symbols* | |
| $h$ | enthalpy (kJ kg -1) |
| $k$ | slope (-) |
| $m$ | mass flow rate (kg s -1) |
| $P$ | pressure (Pa) |
| $Q$ | heat transfer (kJ) |
| $r$ | radius (m) |
| $s$ | entropy (kJ K -1) |
| $T$ | temperature (K) |
| $u$ | internal energy (kJ) |
| $v$ | volume (m 3) |
| $W$ | power (kJ) |
| $x$ | composition (-) |
| $\varepsilon$ | exergy efficiency/thermodynamic perfection degree (-) |
| $\eta$ | thermal efficiency (-) |
| $\vartheta$ | angle between the radius and y-axis (°) |
| $\psi$ | coefficient (-) |
| $\omega$ | angle of variation curve (°) |
| Subscript | |
| C | heat sink |
| con | condenser |
| eva | evaporator |
| ex | exergy |
| global | global parameter |
| H | heat source |
| local | local parameter |
| M | mechanical energy |
| P | thermodynamic perfection degree |
| pum | pump |
| ref | refrigerant |

# This is a paper for the 16th International Conference on Applied Energy (ICAE2024), Sep. 1-5, 2024, Niigata, Japan.

| | |
|---|---|
| sup | superheated degree |
| T | thermal energy |
| total | total energy |
| tur | turbine |

## 1. INTRODUCTION

Energy conversion processes are essential for obtaining electrical energy from fossil fuels and renewable sources. For centuries, a series of design method and optimizations at both the thermodynamic system and thermodynamic processes has been conducted to improve the energy conversion efficiency [1-2]. As a medium for converting thermal energy into mechanical energy, the variation in the thermodynamic state of working fluid plays a decisive role in approaching the upper-limit of energy conversion efficiency [3]. Using Graphical method to visualize the thermodynamic state is considered an effective method for embodying the thermodynamic equations, and it is of great importance in revealing the intrinsic relationships between thermodynamic state parameters.

To visualize the thermodynamic states, six fundamental thermodynamic parameters—temperature (*T*), pressure (*P*), volume (*v*), entropy (*s*), internal energy (*u*), and enthalpy (*h*)—and their internal relationships need to be presented on one diagram. With the extension of application scenarios such as the composition regulation of zeotropic mixture [4], the intermittency and variability of renewable energy sources [5], and finite heat capacity of thermodynamic system [6], the energy conversion processes require more state parameters to describe. Xu et al. proposed a 3D construction method (*T*-*s*-composition *x*) [7], which achieved quantitative description and visualization between thermal energy, chemical energy, and mechanical energy. The projection of 3D volume on *T*-*s*-*x* diagram onto a 2D plane on T-s diagram has been rigorously verified as a Carnot cycle, thus maintaining Gibbs's idea of graphing the ideal cycles as a simple geometry structure [8]. However, this method primarily illustrates the thermodynamic states of the working fluid under steady-state conditions. For systems with dynamic boundary conditions, existing graphical methods tends to present the system performance via the variation of power output over time [5]. As a result, the internal relationship between the thermodynamic states of the working fluid and the system performance fails to connect, limiting the design and optimization of thermodynamic system. Hence, it is necessary to propose a novel graphical method to describe the performance changes of energy conversion systems.

Motivated by the current graphical method's inability to effectively describe the dynamic performance of thermodynamic systems, we proposed an Energy-Energy (*E*-*E*) diagram for the first time in this paper. This graphical method illustrates from a system energy perspective, focusing particularly on the conversion of thermal energy and mechanical energy within the system. The advantages can be summarized as follows: (1) Thermodynamic performance parameters related to the 1st Law of Thermodynamics (energy conservation) and the 2nd Law of Thermodynamics (exergy efficiency $\boldsymbol{\varepsilon_{ex}}$, thermodynamic perfection degree $\boldsymbol{\varepsilon_{p}}$ and thermal efficiency $\boldsymbol{\eta}$) can be simultaneously graphic on the *E*-*E* diagram; (2) The global exergy efficiency ($\boldsymbol{\varepsilon_{ex,global}}$) and the local exergy efficiency ($\boldsymbol{\varepsilon_{ex,local}}$) of the system throughout the energy conversion process can be dynamically illustrated. The detailed principles of the *E*-*E* diagram are described in Section 2. To demonstrate the potential of illustrative applications, a mathematical of a Carnot cycle and an organic Rankine cycle (ORC) with a finite heat source and heat sink scenario is established in Section 3. Subsequently, the dynamic system performance of ORC is analyzed through the *E*-*E* diagram in Section 4.

## 2. METHODOLOGY OF THE *E*-*E* DIAGRAM

To enrich the graphical representation of the system performance under dynamic boundary condition, the *E*-*E* diagram is proposed in this paper, as shown in Fig. 1. The *E*-*E* diagram highly correlate with system state, containing both global system state parameters and local system state parameters. The vertical axes and the horizontal axes in *E*-*E* diagram are respectively designated to represent parameters associated with thermal energy ($W_T$)and mechanical energy ($W_M$). The heat source, heat sink, and thermodynamic cycle are regarded as an isolated system in which the total energy ($W_{total}$) remains constant. Based on this consumption, two analogies can be drawn:

(1) Firstly, $W_{total}$ can be analogized to the fixed length of the radius (*r*) of a circle due to the unchanging sum of the conversion energy during the energy conversion process, which corresponds to the 1st Law of Thermodynamics;

(2) Secondly, the rotation angle ($\Delta\vartheta$) from one system state to another can be analogous to the energy conversion process, different $\Delta\vartheta$ represents different

energy conversion efficiency, which corresponds to the 2nd Law of Thermodynamics;

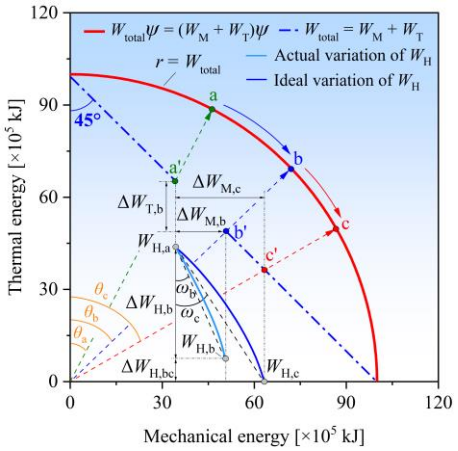


*Fig. 1 Schematic of E-E diagram*

Built on two analogies, the representation of energy conversion on the *E-E* diagram can be presented as a rotation of the radius, where the trajectory of system state variation (state a, b and c) is an arc (**red arc**). It should be noted that the coordinates of x-axis and y-axis are not directly equal to $W_T$ and $W_M$. Instead, they need to be divided by a coefficient ($\psi$) that related to the included angle between the radius and y-axis ($\vartheta$), as shown in Eqs. (1)-(3). The trajectory of the actual energy distribution points (state a', b' and c') in the system forms a straight line with a slope of -1 (**blue dash-and-dot line**). Moreover, a strong geometric correlation can be observed between the red arc and the bule dash-and-dot line for any given state point in the system. For instance, when the system state point is located at state a, the actual energy distribution in the system is at state a', where the centre (0,0), a and a' lie on the same line. Therefore, the tangent of $\vartheta$ is equal to the ratio of two forms of energy within the system, as shown in Eq. (4).

$$W_M = \frac{W_{total}\cos\theta}{\psi} \tag{1}$$

$$W_T = \frac{W_{total}\sin\theta}{\psi} \tag{2}$$

$$\psi = \cos\theta + \sin\theta \tag{3}$$

$$\tan\theta = \frac{W_T}{W_M} \tag{4}$$

According to variation of $\vartheta$ in the *E-E* diagram, the global exergy efficiency ($\varepsilon_{ex,global}$) can be derive using trigonometric function. If points a, b, and c represent the initial state, actual end state, and ideal end state of the energy conversion process system, respectively, $\varepsilon_{ex,global}$ can be expressed as Eq. (5).

$$\varepsilon_{ex,global} = \frac{\sin\left(\theta_c + \frac{\pi}{4}\right)}{\sin\left(\theta_b + \frac{\pi}{4}\right)} \cdot \frac{\sin(\theta_b - \theta_a)}{\sin(\theta_c - \theta_a)} \tag{5}$$

Under a finite heat capacity boundary condition, the temperature of both heat source ($T_H$) and heat sink ($T_C$) continuously vary. The upper limit of energy conversion is reached when $T_H$ equals $T_C$. To provide a more comprehensive description of the energy distribution during the energy conversion process, the variation of the heat source capacity under actual and ideal conditions are also supplemented in Fig. 1, represented by two blue curves. The heat capacity of heat source continually decreases from $W_{H,a}$ to $W_{H,b}$ as energy conversion progresses, whereas the mechanical energy increase from $W_{M,a}$ to $W_{M,b}$. According to the definition, the global thermal efficiency ($\eta_{global}$) is equal the ratio of the variation of mechanical energy ($\Delta W_M$) and heat capacity of heat source ($\Delta W_H$), which is the tangent of $\omega$, as shown in Eq. (6). Moreover, the ratio between $\eta_{global}$ of state b and state c represents the global thermodynamic perfection degree ($\varepsilon_{P,global}$), as shown in Eq. (7).

$$\eta_{global} = \frac{\Delta W_M}{\Delta W_H} = \tan\omega \tag{6}$$

$$\varepsilon_{P,global} = \frac{\tan\omega_b}{\tan\omega_c} \tag{7}$$

For any given state point on the curve, the slope ($k$) equals to the local heat source capacity variation divided by mechanical energy variation, which can be correlated to the local thermal efficiency ($\eta_{local}$), as shown in Eq. (8). Correspondingly, the ratio between $\eta_{local}$ of actual curve and ideal curve represents the local thermodynamic perfection degree ($\varepsilon_{P,local}$), as shown in Eq. (9).

$$\eta_{local} = \lim_{\Delta W \to 0}\left|\frac{\Delta W_M}{\Delta W_T}\right| = -\frac{1}{k_{local}} \tag{8}$$

$$\varepsilon_{P,local} = \frac{k_{ideal}}{k_{actual}} \tag{9}$$

To sum up, the geometry parameters in the *E-E* diagram can be used to comprehensively described the

system performances, and the connection between system performance and geometry parameters are summarized in Table 1.

Table 1 Connection between system performance and geometry parameters

| System performance | | Geometry parameter |
|---|---|---|
| Global parameter | $\varepsilon_{ex,global}$ | $\vartheta_a$, $\vartheta_b$, $\vartheta_c$ |
| | $\eta_{global}$ | $\omega_b$, $\omega_c$ |
| | $\varepsilon_{P,global}$ | $\omega_b$, $\omega_c$ |
| Local parameter | $\eta_{local}$ | $k_{ideal}$, $k_{actual}$ |
| | $\varepsilon_{P,local}$ | $k_{ideal}$, $k_{actual}$ |

## 3. CASE STUDY

In order to exemplify the convenience with which *E-E* diagram reflects the variations depicted in the system's energy distribution, an ORC cycle with a finite heat source and heat sink are chosen as an example to graphically represent the distribution of thermal energy and mechanical energy. Moreover, the graphic representation on the *E-E* diagram under different boundary condition are also compared.

### *3.1 Problem description and mathematical model*

The sum of the ORC system, heat source, and heat sink is viewed as an isolated system, which contains thermal energy ($W_T$) and mechanical energy ($W_M$) with an initial ratio of $W_T$ to $W_M$ at 4:1. Moreover, thermal energy is comprised of two reservoirs (heat source and heat sink) possessing distinct energy potentials. The system schematic and the summary of initial conditions are shown in Fig. 2 and Table 2. According to these initial temperatures of heat source and heat sink, R245fa is selected as the working fluid. Under actual working conditions. To balance the heat exchange area with the temperature difference between the heat medium and working fluid, the pinch point temperature difference (PPTD) with the working fluid is set to 5-10 K.

Table 2 System initial conditions

| Parameters | Number |
|---|---|
| Initial total energy $W_{total}$ (kJ) | $1\times10^6$ |
| Initial mechanical energy $W_{M,a}$ (kJ) | $2\times10^5$ |
| Initial thermal energy $W_{T,a}$ (kJ) | $8\times10^5$ |
| Initial heat source $W_{H,a}$ (kJ) | $6.4\times10^5$ |
| Initial heat sink $W_{C,a}$ (kJ) | $1.6\times10^5$ |
| Pinch point temperature difference PPTD (K) | 5-10 |
| Superheated temperature $\Delta T_{sup}$ (K) | 5 |
| Mass flow rate of heat source $\dot{m}_H$ (kg/s) | 20 |
| Mass flow rate of heat sink $\dot{m}_C$ (kg/s) | 40 |

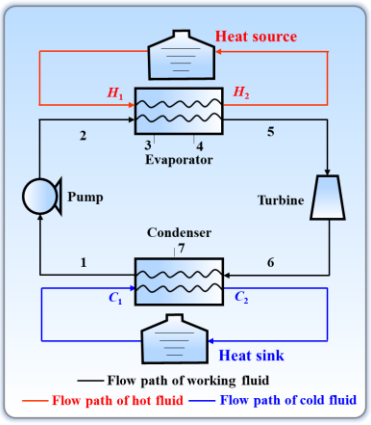


*Fig. 2 Schematic of organic Rankine cycle (ORC)*

In ORC, the thermodynamic state of working fluid varies at each thermodynamic processes, the energy balance equations can be shown in Eqs. (10)-(13). Moreover, in actual conditions, the exergy loss existing in each thermodynamic processes due to the irreversible factor, thereby decreasing the conversion mechanical energy. However, ideally, the system entropy ($S_{system}$) is keeping as constant under the whole energy conversion process.

$$Q_{eva} = \dot{m}_{ref}\left(h_5 - h_2\right) \tag{10}$$

$$W_{tur} = \dot{m}_{ref}\left(h_6 - h_5\right)\eta_{turbine} \tag{11}$$

$$Q_{con} = \dot{m}_{ref}\left(h_6 - h_1\right) \tag{12}$$

$$W_{pum} = \frac{\dot{m}_{ref}\left(h_2 - h_1\right)}{\eta_{pum}} \tag{13}$$

### *3.2 Solution algorithm*

As the progress of energy conversion, the boundary condition of ORC is dynamic varies, thus the conversion time ($t$) needed to be discretized. In this study, the length of each time step ($\Delta t$) and the absorbing heat of working fluid are setting as 10 s and 400 kJ respectively. Moreover, after each time step ($i$), the heat exchange medium from heat source/heat sink flows back to the reservoir after exchanging heat with working fluid and mixes with the internal fluid before flowing out again. Therefore, the temperature of heat source and heat sink varies at different time step. As the temperature

difference between the heat source and the heat sink is within 25 K, the energy conversion efficiency of system reaches the upper limit.

## 4. RESULTS AND DISCUSSION

In a finite heat capacity system, the upper limit of energy conversion is largely determined by the irreversible loss of each component in ORC. The lower the irreversible loss, the higher the conversion mechanical energy, which also can be intuitively present through the *E-E* diagram. In this section, two systems with different isentropic efficiency of 30% (Case A) and 85% (Case B) under the same boundary conditions are selected for analysis. The temperature of heat source and heat sink are setting as 423.15 K and 278.15 K, respectively. The graphical expression of system energy conversion process is shown in Fig. 3.

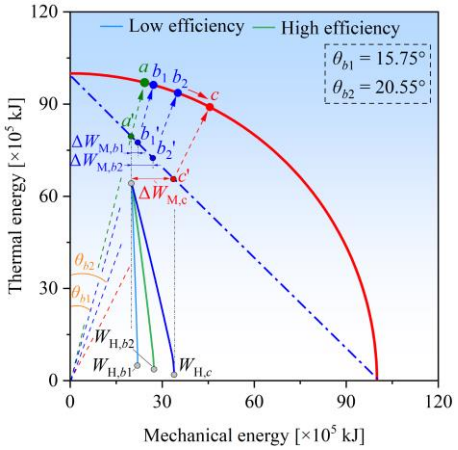


*Fig. 3 E-E* diagram representation at different isentropic efficiency

Under actual working condition, the initial mechanical energy ($W_{M,a}$) and the initial thermal energy ($W_{T,a}$) are $2\times10^5$ kJ and $8\times10^5$ kJ, respectively. As the system reaches the upper limit of energy conversion (State $b_1$ and $b_2$), the mechanical energy in Case A ($W_{M,b1}$) and Case B ($W_{M,b2}$) are $2.20\times10^5$ kJ and $2.73\times10^5$ kJ respectively. Correspondingly, the thermal energy in these cases, $W_{T,b1}$ and $W_{M,b2}$, are $7.80\times10^5$ kJ and $7.27\times10^5$ kJ, respectively. Furthermore, due to varying isentropic efficiency, the releasing heat from working fluid to the heat sink is differs, resulting in end temperature of 332.82 K in Case A and 319.55 K in Case B. Consequently, the heat capacity variation of heat source in Case A ($W_{H,b1}$) is lower than in Case B ($W_{H,b2}$). However, under ideal working condition, the mechanical energy ($W_{M,c}$) and the thermal energy ($W_{T,c}$) are $33.83\times10^5$ kJ and $66.17\times10^5$ kJ, respectively. Thus, the working fluid will absorb more thermal energy from the heat source ($W_{H,c}$), equating to $62.08\times10^5$ kJ.

Based on different system states, the geometric parameters on the *E-E* diagram vary, as summarized in Table 3. It can be observed that the constraint of isentropic efficiency results in different endpoints for system states $b_1$ and $b_2$. The higher the rotation angle within the same boundary conditions, the higher the global exergy efficiency ($\varepsilon_{ex,global}$). At low isentropic efficiency, the rotation angle ($\vartheta_{b1}$) is 15.75°, at which point the system gains mechanical energy $\Delta W_{M,b1}$. However, the rotation angle ($\vartheta_{b2}$) under high isentropic efficiency can reach 20.55°, where the mechanical energy increase is $\Delta W_{M,b2}$. The exergy efficiency of the energy conversion process can be determined from the change in $\vartheta$ using Eq. (5), which are 14.43% in Case A and 52.51% in Case B, respectively. Additionally, based on the variation in $\omega$, the global thermal efficiency ($\eta_{global}$) and global thermodynamic perfection ($\varepsilon_{P,global}$) can be calculated using Eqs. (6)-(7). $\eta_{global}$ for Case A, Case B, and the ideal condition are 3.38%, 12.07%, and 22.28%, respectively. Meanwhile, $\varepsilon_{P,global}$ for Case A and Case B are 15.16% and 54.18%, respectively. During energy conversion, at the beginning ($i$ = 1), the thermal efficiency ($\eta_{local}$) under high isentropic efficiency is 17.95%, with the local exergy efficiency ($\varepsilon_{ex,local}$) reaching 55.03%. As the energy conversion progresses, the decreasing temperature difference between the heat source and the heat sink results in a decrease in thermal efficiency, leading to higher cumulative exergy loss compared to the ideal case. At $i$ = 93, $\eta_{local}$ is only 1.01%, and the corresponding $\varepsilon_{ex,local}$ decreases to 9.69%, indicating that more thermal energy is required to convert the same amount of mechanical energy.

Table 3 Angle of each geometry parameters

| Parameters | Angle | Parameters | Angle |
|---|---|---|---|
| $\vartheta_a$ | 14.03° | $\omega_{b1}$ | 1.96° |
| $\vartheta_{b1}$ | 15.75° | $\omega_{b2}$ | 6.92° |
| $\vartheta_{b2}$ | 20.55° | $\omega_c$ | 12.56° |
| $\vartheta_c$ | 27.08° | | |

In summary, under the same boundary conditions, when the two systems operate with different energy efficiency, the higher the $\vartheta$, the higher the $\varepsilon_{ex,global}$. Similarly, the higher the $\omega$, the higher the $\eta_{local}$ and the $\varepsilon_{ex,local}$. Therefore, compared with *T-s* diagram, which uses the area ratio to display the system performance, the comparison of the conversion efficiency between different systems through the angle of *E-E* diagram is easier, especially the system performance under the dynamic boundary.

## 5. CONCLUSIONS

In this study, a new graphical expression method based on thermodynamic process parameters is proposed. The principle and methodology of Energy-Energy diagram (*E*-*E*) are introduced. A case study of thermal energy conversion to mechanical energy under finite heat capacity is conducted mathematically. The main conclusions are as follows:

(1) To address the difficulty of graphically representing dynamic performance variations in the energy conversion process system using thermodynamic state parameters, the graphical representation of *E*-*E* diagram is proposed;

(2) The *E*-*E* diagram not only represents the parameters related to the 1st and 2nd Laws of Thermodynamics but also presents the global and local system performance;

(3) For two systems with different isentropic efficiency, the *E*-*E* diagram can intuitively present the differences in performance between two system;


## ACKNOWLEDGEMENT

There is no funding for this article.


## REFERENCE


[1] Xu W, Deng S, Zhao L, et al. Performance analysis on novel thermodynamic cycle under the guidance of 3D construction method. Appl Energ 2019;250:478-492.

[2] Wang X, Liu Q, Bai Z, et al. Thermodynamic investigations of the supercritical CO2 system with solar energy and biomass. Appl Energ 2018;227:108-118.

[3] Clapeyron É. MÉmoire sur la puissance mortice de la chaleur. Journal De L'École Polytechnique 1834;23:153-190.

[4] Xu W, Zhao R, Deng S, et al. Is zeotropic working fluid a promising option for organic Rankine cycle: A quantitative evaluation based on literature data. Renew Sust Energy Rev 2021;148:111267.

[5] Zantye MS, Gandhi A, Wang Y, et al. Optimal design and integration of decentralized electrochemical energy storage with renewables and fossil plants. Energ Environ Sci 2022;15:4119-4136.

[6] He D, Tang X, Rehan MA, et al. A novel high-efficient continuous power generation device employing thermally regenerative electrochemical cycle. Appl Therm Eng 2024;236:121879.

[7] Xu W, Zhao L, Deng S, et al. A preliminary approach to the 3D construction of thermodynamic cycle based on zeotropic working fluids. Chinese Sci Bull 2019;64:206-214.

[8] Gibbs JW. The collected works of J. Willard Gibbs: Thermodynamics. Longmans, Green and Company; 1928.